The Astrophysical Journal Supplement Series, 188:500–505, 2010 June doi:10.1088/0067-0049/188/2/500

FOURIER TRANSFORM EMISSION SPECTROSCOPY OF THE $A\ ^2\Pi$–$X\ ^2\Sigma^+$ (RED) SYSTEM OF $^{13}C^{14}N$

R. S. Ram[1], L. Wallace[2], K. Hinkle[2], and P. F. Bernath[1,3,4]
[1] Department of Chemistry, University of Arizona, Tucson, AZ 85721, USA
[2] National Optical Astronomy Observatories, Tucson, AZ 85726, USA
[3] Department of Chemistry, University of Waterloo, Waterloo, Ontario N2L 3G1, Canada
[4] Department of Chemistry, University of York, Heslington, York, YO10 5DD, UK
Received 2010 March 23; accepted 2010 May 5; published 2010 June 3

ABSTRACT

Emission spectra of the $A\ ^2\Pi$–$X\ ^2\Sigma^+$ transition (red system) of $^{13}C^{14}N$ have been measured in the 4000–15,000 cm^{-1} region using the Fourier transform spectrometer associated with the McMath–Pierce Solar Telescope of the National Solar Observatory. The $^{13}C^{14}N$ free radical was produced in microwave discharge of a mixture of $^{13}CH_4$ and $^{14}N_2$. Rotational analysis of 22 vibrational bands involving vibrational levels up to $v' = 8$ and $v'' = 5$ of the excited and ground states has been obtained and much improved spectroscopic constants have been determined. An experimental line list and calculated term values are provided. The results of the present analysis are useful for the identification of $^{13}C^{14}N$ lines in late-type stars in the red and near-infrared spectral regions.

Key words: ISM: molecules – line: identification – methods: laboratory – molecular data – stars: carbon

Online-only material: supplemental data files (tar.gz)

1. INTRODUCTION

CN is an important free radical in chemistry and astronomy. The chemical kinetics (Titarchuk & Halpern 1995; North et al. 1997; Antipov et al. 2009), flame diagnostics (Hirano & Tsujishita 1994; Mercier et al. 2001) and collisional processes (Chen & Heaven 2000; Tamaoki et al. 2005; Peach et al. 2008; Khachatrian & Dagdigian 2009) have all been studied for CN. The ubiquity of CN in astronomical objects makes CN a key probe of carbon and nitrogen abundance and isotopic ratios. The CN radical has been observed, for instance, in comets (Johnson et al. 1983; Fray et al. 2005), solar and stellar atmospheres (Lambert et al. 1984), circumstellar shells (Wootten et al. 1982; Wiedemann et al. 1991), the interstellar medium (Turner & Gammon 1975; Meyer & Jura 1985), and the integrated light of galaxies (Riffel & Pastoriza 2007). Applications span topics from the origin and abundances of the elements (Lambert 1968; Smith et al. 2002), the temperature of the microwave background radiation (Roth et al. 1993), the star formation process (Wang et al. 2004; Riffel & Pastoriza 2007), to the origin of galaxies (Banerji et al. 2009).

The spectrum of CN has been studied in the laboratory from the microwave through the ultraviolet. This paper is on the electronic spectrum in the optical and near-IR. The electronic spectra of the main isotopologue $^{12}C^{14}N$ have been studied in detail for many years. The $A\ ^2\Pi$–$X\ ^2\Sigma^+$ (red) and the $B\ ^2\Sigma^+$–$X\ ^2\Sigma^+$ (violet) systems are important transitions for astronomy. Most electronic transitions of molecules of astrophysical interest occur in the blue and ultraviolet. However, for CN detectable red system lines extend as far red as the 2.0–2.5 μm K band. The presence of CN red system lines through the red and into the near-infrared is one of the features that makes this system a useful astronomical probe. For instance, the red system lines can be studied in objects which have their peak flux in the infrared or which are heavily reddened. CN red system lines can also be selected near lines of other astrophysically important molecules found in the near-infrared, for instance CO or OH.

References to the previous studies of the $A\ ^2\Pi$–$X\ ^2\Sigma^+$ (red) and the $B\ ^2\Sigma^+$–$X\ ^2\Sigma^+$ (violet) systems can be found in recent papers: for the red system Prasad & Bernath (1992a) and Rehfuss et al. (1992) and for the violet system Prasad & Bernath (1992b), Rehfuss et al. (1992), and Ram et al. (2006). More recently, several additional papers on the $A\ ^2\Pi$–$X\ ^2\Sigma^+$ transition have appeared including concentration modulation laser spectroscopy of the 2–0 band by Liu et al. (2001), time-resolved Fourier transform spectroscopy of seven bands belonging to the $\Delta v = -3$ sequence by Civiš et al. (2008), and sub-Doppler Stark spectroscopy of the 1–0 band by Hause et al. (2009). Horká et al. (2004) have published on the observation and analysis of vibration–rotation bands in the $\Delta v = 1$ sequence from 1–0 to 9–8.

In spite of much work on the electronic spectra of the main isotopologue, relatively little data are available for $^{13}C^{14}N$, and no high-resolution electronic observations have been reported for $^{12}C^{15}N$ and $^{13}C^{15}N$. There are obvious applications for these spectral lines, for instance in determining isotopic ratios. In addition, as spectrum synthesis becomes increasingly sophisticated and sensitive tool for determining abundances, it is increasingly important to include possible blending of features in the line list. Since values of $^{12}C/^{13}C$ smaller than four have been determined in astronomical objects (Lambert et al. 1984), a detailed line list for $^{13}C^{14}N$ is required.

The previous work on $^{13}C^{14}N$ includes the rotational analysis of the 0–0, 0–1, and 0–2 bands of the $B\ ^2\Sigma^+$–$X\ ^2\Sigma^+$ system by Jenkins & Wooldridge (1938), and the 2–0 and 3–0 bands of the $A\ ^2\Pi$–$X\ ^2\Sigma^+$ system by Wyller (1966). Fay & Wyller (1970) stress the need for high-resolution measurements of the $^{13}C^{14}N$ red system bands near 1 μm and to longer wavelengths. Hosinsky & Lindgren (1976) measured high-resolution spectra of the 0–0, 1–0, and 2–1 bands of the $A\ ^2\Pi$–$X\ ^2\Sigma^+$ system of $^{13}C^{14}N$ and in a subsequent paper this group reported the analysis of the 0–0, 1–0, 2–1, 3–2, 2–0, 3–1, and 4–2 bands (Hosinsky et al. 1982). From the spectroscopic constants obtained in these studies they extrapolated the 0–0 band up to $J = 75.5$ to better match stellar temperatures. A line list currently in common use is that of Plez, discussed in Hill et al. (2002). This draws data from eight separate sources. Garcia-Hernandez et al. (2009) point out the inadequacies of this list for $^{13}C^{14}N$.

Millimeter wave spectra of $^{13}C^{14}N$ radical have been measured in the laboratory in two previous studies (Bogey et al. 1984, 1986). In the first study, the $N = 0 \rightarrow 1$ and $N = 1 \rightarrow 2$ transitions were observed in a radio frequency glow discharge source (Bogey et al. 1984) while in a subsequent study they observed the millimeter wave spectrum of higher vibrational levels up to $v = 9$ (Bogey et al. 1986). These observations, in conjunction with previous measurements on $^{12}C^{14}N$, were used to obtain the vibrational and isotopic dependence of molecular constants. In a more recent study, infrared laser spectroscopy was used to observe the fundamental 1–0 bands of $^{12}C^{14}N$ and $^{13}C^{14}N$ in their ground ($^2\Sigma^+$) states by Hempel et al. (2003), and Hübner et al. (2005) reported the fundamental bands of the four isotopologues $^{12}C^{14}N$, $^{13}C^{14}N$, $^{12}C^{15}N$, and $^{13}C^{15}N$ using tunable diode laser absorption spectroscopy.

In the present work we have measured high-resolution spectra of the $^{13}C^{14}N$ radical in the 4000–15000 cm^{-1} region from the high-resolution spectra recorded with a Fourier transform spectrometer. In total, 22 bands of the $A\ ^2\Pi$–$X\ ^2\Sigma^+$ transition involving vibrational levels $v'' = 0$–5 and $v' = 0$–8 have been measured and rotationally analyzed. An extensive set of spectroscopic constants and rotational line positions are reported for $^{13}C^{14}N$ after the analysis of these bands. A similar analysis for $^{12}C^{14}N$ is reported by Ram et al. (2010).

2. EXPERIMENTAL DETAILS

The spectra used in the present analysis were recorded by J. Brault and R. Engleman at the National Solar Observatory located at Kitt Peak in 1977 and 1992. The molecules were produced in a microwave discharge lamp by exciting a mixture of argon, $^{14}N_2$, and a trace of $^{13}CH_4$. Two sets of experiments were performed, one using normal $^{14}N_2$ in the discharge (1977 experiments) and the other using active nitrogen (1992 experiments). The spectra were recorded using the Fourier transform spectrometer associated with McMath–Pierce Solar Telescope. In both cases the spectra were recorded in two parts. In the 1977 experiments, the 2900–12000 cm^{-1} region was recorded using GaAs filters, visible beam splitter, and InSb detectors, and the 8000–22000 cm^{-1} region was recorded using GG475 filters, visible beam splitter, and Si photodiode detectors. In these experiments, the spectra were recorded at respective resolutions of 0.015 cm^{-1} and 0.03 cm^{-1}, by co-adding seven and eight scans, respectively. In the 1992 experiments with active nitrogen, the 2900–16000 cm^{-1} region was recorded using the CaF_2 beamsplitter, InSb detectors, and RG610 filters and in the other experiment the 9000–31000 cm^{-1} region was recorded using the UV beam splitter and midrange Si photodiode detectors. In the two experiments, the spectra were recorded at respective resolutions of 0.016 cm^{-1} and 0.03 cm^{-1}, by co-adding five and four scans, respectively. Only a trace of $^{12}C^{14}N$ was found in the 1977 spectra while the 1992 spectra are free from $^{12}C^{14}N$ impurity. In addition to several N_2 bands, some $^{12}C^{16}O$ and $^{13}C^{16}O$ 2–0 overtone vibration–rotation lines near 4000 cm^{-1} were observed in the 1977 spectra while some $^{13}C^{16}O$ 2–0 vibration–rotation lines were observed very weakly in the 1992 spectra.

The line positions were extracted from the observed spectra using a data reduction program called PC-DECOMP developed by J. Brault. The peak positions were determined by fitting a Voigt line shape function to each spectral feature. The $^{12}C^{16}O$ and $^{13}C^{16}O$ lines were used for calibration of the spectrum near 4000 cm^{-1} by using the CO measurements provided by Maki & Wells (1995). The spectra in the 5000–15000 cm^{-1} region were calibrated using the Ar line measurements by Whaling et al. (2002) as corrected by Sansonetti (2007). After calibration our two sets of spectra were brought to the same scale by transferring the calibration using common molecular lines. The precision of measurement is expected to be better than ± 0.002 cm^{-1} for the stronger and unblended lines. However, there is overlapping by satellite branches for lower J transitions in some branches resulting in somewhat higher uncertainty for some rotational lines.

3. OBSERVATIONS

The observed spectra are full of bands in the 4000–30000 cm^{-1} range belonging to the $A\ ^2\Pi$–$X\ ^2\Sigma^+$ (4000–20000 cm^{-1}) and $B\ ^2\Sigma^+$–$X\ ^2\Sigma^+$ (20000–30000 cm^{-1}) transitions of $^{13}C^{14}N$. In the present work, we have rotationally analyzed 22 bands of the $A\ ^2\Pi$–$X\ ^2\Sigma^+$ transition located in the 4000–15000 cm^{-1} region. These bands involve vibrational levels up to $v' = 8$ and $v'' = 5$ of the upper and lower states, respectively. The higher wavenumber bands (lying at >15000 cm^{-1}) remain unassigned and probably involve even higher vibrational levels. The principal goal of the present work is to obtain measurements of bands belonging to the $\Delta v = -1$ and -2 sequences of $^{13}C^{14}N$ in order to assign lines in the 4000–10000 cm^{-1} wavenumber region of stellar spectra. We have analyzed a number of bands belonging to the $\Delta v = -2$, -1, 0, 1, 2, 3, and 4 sequences, the details of which are provided in the following sections.

3.1. The $\Delta v = -2$ Sequence

The bands located in the 4000–5200 cm^{-1} region belong to the $\Delta v = -2$ sequence, which is the weakest of the observed sequences of the red system. We have assigned rotational lines belonging to the 0–2, 1–3, 2–4, and 3–5 bands. All 12 expected branches have been identified in most of the stronger bands. A portion of the 0–2 band is provided in Figure 1 with some R_2 and Q_{21} rotational lines near the R_2 head marked. We have identified rotational lines up to $J = 52.5$ in the strong branches of this band. The satellite branches arising due to the spin splitting in the ground state are well resolved as can be seen in Figure 1. We have identified rotational lines up to $J = 45.5$ in the 1–3 band and up to $J = 36.5$ in the 2–4 band. The 3–5 band is the weakest and only four branches could be identified. The upper state rotational constants obtained from rotational analysis of other bands with $v' = 3$ and the available millimeter wave measurements for the $v'' = 5$ vibrational level of the ground state (Bogey et al. 1986) were helpful in the assignment. The $\Delta v = -2$ sequence bands were not measured in previous studies.

3.2. The $\Delta v = -1$ and 0 Sequences

The bands belonging to the $\Delta v = -1$ sequence are located in the 6000–7200 cm^{-1} region. This sequence is the strongest sequence in our spectrum below 10000 cm^{-1} and in fact is stronger than the 0–0 band. We have identified rotational lines belonging to the 0–1, 1–2, and 2–3 bands. The 0–1 band is strongest in intensity and we have identified rotational lines up to $J = 82.5$. Although the 1–2 and 2–3 bands are weaker than the 0–1 band, we were able to assign rotational lines up to $J = 67.5$ and 53.5. The 3–4 band is also present in our spectra but is much weaker. This band is overlapped by a much stronger N_2 band; therefore we did not attempt to obtain a rotational analysis. No measurements of the bands belonging to the $\Delta v = -1$ sequence of $^{13}C^{14}N$ have been carried out in any previous studies.

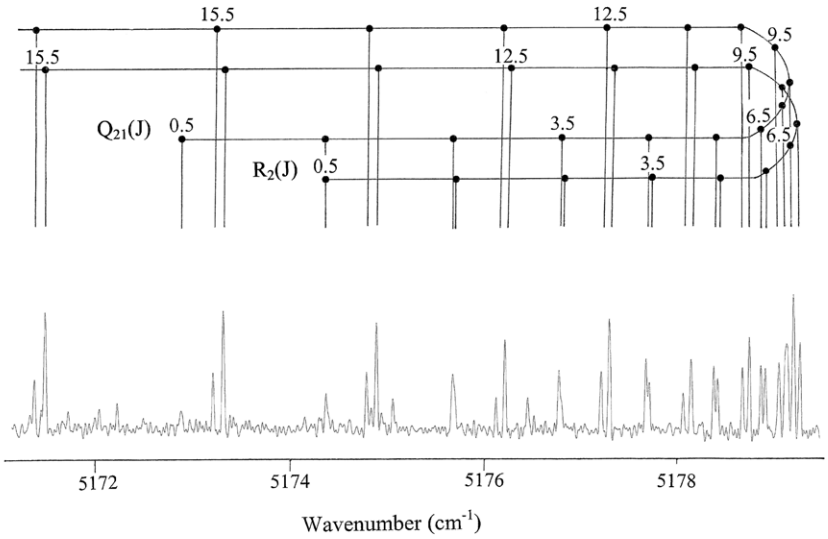

Figure 1. A portion of the spectrum of the 2–0 band of $^{13}C^{14}N$ near the R_2 head. Some rotational lines in the main (R_2) and satellite (Q_{21}) branches have been marked.

Only the 0–0 band belonging to the $\Delta v = 0$ sequence was measured and rotationally analyzed. Although the 1–1 band is weakly seen in our spectra near the band head, the 2–2 and other higher vibrational bands are much weaker and no attempt was made to analyze them. If needed, the rotational lines in these bands can easily be predicted using the rotational constants or term values obtained from other bands. For the 0–0 band we have identified rotational lines up to $J = 75.5$ in the stronger branches. Rotational analysis of this band was reported previously by Hosinsky & Lindgren (1976) and Hosinsky et al. (1982).

3.3. The $\Delta v = 1$ and 2 Sequences

We have obtained the rotational analysis of the 1–0, 2–1, and 3–2 bands in the $\Delta v = 1$ sequence and the 2–0, 3–1, and 4–2 bands in the $\Delta v = 2$ sequence. These bands were previously measured at grating resolution by Hosinsky & Lindgren (1976) and Hosinsky et al. (1982). We have measured all 12 branches in most of the bands up to much higher J values than in the previous work. For example, we have measured rotational lines up to $J = 82.5$, 72.5, 48.5 in the 1–0, 2–1, and 3–2 compared to the previous measurements up to $J = 33.5$, 35.5, 27.5, respectively. Similarly we have identified higher J rotational lines and more branches in the $\Delta v = 2$ sequence. For example, we observed rotational lines up to $J = 52.5$ in the 4–2 band compared to $J = 28.5$ observed by Hosinsky et al. (1982).

3.4. The $\Delta v = 3$ and 4 Sequences

We have measured the rotational structure in the 3–0, 4–1, 5–2, 6–3, 7–4, and 8–5 bands of the $\Delta v = 3$ sequence and 7–3 and 8–4 bands of the $\Delta v = 4$ sequence. The 3–0 and 4–1 bands were measured from the discharge using normal $^{14}N_2$, while the other higher vibrational bands were measured using active nitrogen. As mentioned earlier, the spectrum recorded using active nitrogen results in the observation of extensive sequence bands with higher vibrational levels. Similar observations were made for the $^{12}C^{14}N$ red system in active nitrogen where bands were observed with vibrational levels up to $v' = 22$ and $v'' = 12$ (Ram et al. 2010). As noted in the case of $^{12}C^{14}N$, bands observed with active nitrogen result in high vibrational excitation but with low rotational excitation. For example, for bands with $v' = 5$–8 of the $A\ ^2\Pi$ state observed in active nitrogen, the rotational observations were limited to $J \leqslant 25.5$. We have observed perturbations affecting the rotational lines with $J' > 21.5$ of the $^2\Pi_{1/2,f}$ spin component and $J' > 11.5$ $^2\Pi_{3/2,f}$ spin component of the $v' = 8$ vibrational level. All rotational lines affected by perturbations were given lower weights. No analyses of the bands with $v' = 5$–8 vibrational levels of the $A\ ^2\Pi$ state of $^{13}C^{14}N$ were reported in previous studies.

4. ANALYSIS AND DISCUSSION

We have identified all 12 branches in most of the strong bands. The analysis was accomplished by comparing the combination differences from common vibrational bands. The spectroscopic constants were determined by fitting the observed line positions in different bands using Brown's Hamiltonian (Brown et al. 1979). The matrix elements for the $A\ ^2\Pi$ and $X\ ^2\Sigma^+$ states are provided, for example, in a paper by Amiot et al. (1981). The rotational lines were given weights based on their signal-to-noise ratio and extent of blending. The lines for which main and satellite branches are unresolved were also given reduced weights. In the final fit, the lines of all the bands of the red system were combined together and fitted simultaneously.

The available microwave and submillimeter wave measurements (Bogey et al. 1984, 1986) and near-infrared vibration–rotation measurements by Hempel et al. (2003) and Hübner et al. (2005) were also included in our data. For the 1–0 vibration–rotation band the measurements were given lower weights than quoted in the papers (Hempel et al. 2003; Hübner et al. 2005), since the reported rotational line positions are the average of the two spin doublets (although the splitting was partly resolved for many of the lines).

The observation of high-J rotational lines enables us to determine higher order constants. For example, we have determined the spectroscopic constants T_v, B_v H_v, and γ_v for $v'' = 0$, 1, 2, and 3 of the ground state, although H_v was not determined for these levels by Bogey et al. (1986) in their submillimeter wave study. For the excited state the constants T_v, A_v, A_{Dv}, A_{Hv} B_v, D_v, H_v, q_v, q_{Dv}, p_v, and p_{Dv} are required for most of the vibrational levels. The constants obtained for the ground and excited states of $^{13}C^{14}N$ are provided in Tables 1 and 2, respectively. The spectroscopic constants obtained in this work agree very well with those reported by Hosinsky & Lindgren (1976) and Hosinsky et al. (1982), but are more precise.

Table 1
Spectroscopic Constants (in cm^{-1}) for the $A\ ^2\Pi$ State of $^{13}C^{14}N$

Constants	$v = 0$	$v = 1$	$v = 2$	$v = 3$	$v = 4$
T_v	9118.238633(50)	10868.954190(58)	12595.157043(65)	14296.841741(75)	15973.99399(11)
A_v	−52.65542(10)	−52.58401(11)	−52.51017(12)	−52.43420(17)	−52.35574(24)
$A_{D_v} \times 10^4$	−2.0096(29)	−1.9985(31)	−1.9667(36)	−1.9318(57)	−1.957(10)
$A_{H_v} \times 10^7$	0.04734(43)	0.05382(44)	0.06099(59)	0.0754(13)	0.1185(24)
B_v	1.63639759(13)	1.62018703(14)	1.60393531(18)	1.58763374(19)	1.57129000(30)
$D_v \times 10^6$	5.63645(15)	5.64598(15)	5.65771(18)	5.665879(68)	5.67939(12)
$H_v \times 10^{12}$	1.657(22)	1.266(23)	1.068(27)	...	...
$q_v \times 10^4$	−3.5963(12)	−3.6667(12)	−3.7467(14)	−3.8197(23)	−3.9270(51)
$q_{D_v} \times 10^8$	0.9676(32)	1.0260(32)	1.1050(43)	1.134(10)	1.285(23)
$p_v \times 10^3$	8.0973(57)	8.0595(62)	8.0655(71)	8.015(10)	8.001(21)
$p_{D_v} \times 10^7$	−2.720(21)	−2.860(23)	−3.271(31)	−3.445(65)	−4.11(12)
Constants	$v = 5$	$v = 6$	$v = 7$	$v = 8$	
T_v	17626.60533(16)	19254.66288(25)	20858.15241(19)	22437.09699(30)	
A_v	−52.27964(36)	−52.21266(55)	−52.16549(39)	−52.25872(57)	
$A_{D_v} \times 10^4$	−1.905(19)	−1.770(73)	−1.940(45)	1.16(10)	
$A_{H_v} \times 10^7$	0.1800(61)	0.486(91)	1.495(48)	2.57(14)	
B_v	1.55490804(62)	1.5384615(28)	1.5219892(18)	1.5056223(47)	
$D_v \times 10^6$	5.69593(35)	5.7081(65)	5.7128(35)	5.523(15)	
$q_v \times 10^4$	−3.986(11)	−4.201(21)	−4.389(11)	−8.70(15)	
$q_{D_v} \times 10^6$	0.01235(71)	...	...	1.064(39)	
$p_v \times 10^2$	0.7928(34)	0.7735(41)	0.7800(24)	1.348(10)	
$p_{D_v} \times 10^7$	−5.28(29)	...	...		

Note. Numbers quoted in parentheses are one standard deviation error in the last digits.

Table 2
Spectroscopic Constants (in cm^{-1}) for the $X\ ^2\Sigma^+$ State of $^{13}C^{14}N$

Constants	$v = 0$	$v = 1$	$v = 2$
T_v	0.0	2000.085127(44)	3974.971248(48)
B_v	1.812691739(29)	1.796343168(29)	1.779944749(29)
$D_v \times 10^6$	5.87699(15)	5.88542(14)	5.89425(16)
$H_v \times 10^{12}$	3.564(23)	3.412(22)	3.165(30)
$\gamma_v \times 10^3$	6.95466(20)	6.87872(20)	6.79452(20)
	$v = 3$	$v = 4$	$v = 5$
T_v	5924.620809(68)	7848.994923(95)	9748.05460(19)
B_v	1.763494607(30)	1.746990598(30)	1.730430475(30)
$D_v \times 10^6$	5.90590(25)	5.91223(25)	5.92571(60)
$H_v \times 10^{12}$	3.49(10)	...	...
$\gamma_v \times 10^3$	6.70004(20)	6.59137(20)	6.46270(20)

Note. Numbers quoted in parentheses are one standard deviation error in the last digits.

Table 3
Equilibrium Constants (in cm^{-1}) for the $A\ ^2\Pi$ State of $^{13}C^{14}N$

Constants	$A\ ^2\Pi$
T_e	9243.17433(85)
ω_e	1775.2160(15)
$\omega_e x_e$	12.24779(63)
$\omega_e y_e$	−0.001680(75)
A_e	−52.6870(18)
α_{A1}	0.0615(25)
α_{A2}	0.00503(89)
α_{A3}	−0.000523(83)
B_e	1.64448513(96)
$\alpha_1 \times 10^2$	−1.616436(97)
$\alpha_2 \times 10^5$	−2.249(20)
r_e (Å)	1.23304088(36)

Note. Values in parentheses are one standard deviation uncertainties in the last digits.

The main spectroscopic constants of the ground and excited states vary smoothly with v except for the constants for the $v = 8$ vibrational level of the $A\ ^2\Pi$ state which is affected by perturbation. A list of all of the measurements used in the determination of the spectroscopic constants and the obs.–calc. residuals is provided in the electronic Supplement 1. The final spectroscopic constants were used to calculate the term values for the observed vibrational levels of the $X\ ^2\Sigma^+$ and $A\ ^2\Pi$ states, which are provided in the electronic Supplement 2. The term values have been extrapolated to a few higher J rotational levels than the observed ones for each vibrational level.

These constants have been used to evaluate equilibrium constants for the $A\ ^2\Pi$ and $X\ ^2\Sigma^+$ states using the following expressions:

$$G(v) = \omega_e(v + 1/2) - \omega_e x_e(v + 1/2)^2 + \omega_e y_e(v + 1/2)^3 + \omega_e z_e(v + 1/2)^4 \quad (1)$$

$$A_v = A_e + \alpha_{A1}(v + 1/2) + \alpha_{A2}(v + 1/2)^2 + \alpha_{A3}(v + 1/2)^3 \quad (2)$$

$$B_v = B_e + \alpha_1(v + 1/2) + \alpha_2(v + 1/2)^2 + \alpha_3(v + 1/2)^3 \quad (3)$$

$$\gamma_v = \gamma_e + \gamma_1(v + 1/2) + \gamma_2(v + 1/2)^2 \quad (4)$$

Because of the presence of some perturbations in the $v = 8$ vibrational level of the $A\ ^2\Pi$ state, the values corresponding to this vibrational level were given much lower weights when fitting for the equilibrium constants for the $A\ ^2\Pi$ state. The equilibrium constants for the two states are provided in Tables 3 and 4. The present equilibrium constants also agree well with the equilibrium constants of Hosinsky & Lindgren (1976) and Hosinsky et al. (1982). The equilibrium rotational constants B_e derived for the $A\ ^2\Pi$ and $X\ ^2\Sigma^+$ states (Tables 3 and 4) have been used to determine the equilibrium bond length (r_e) of

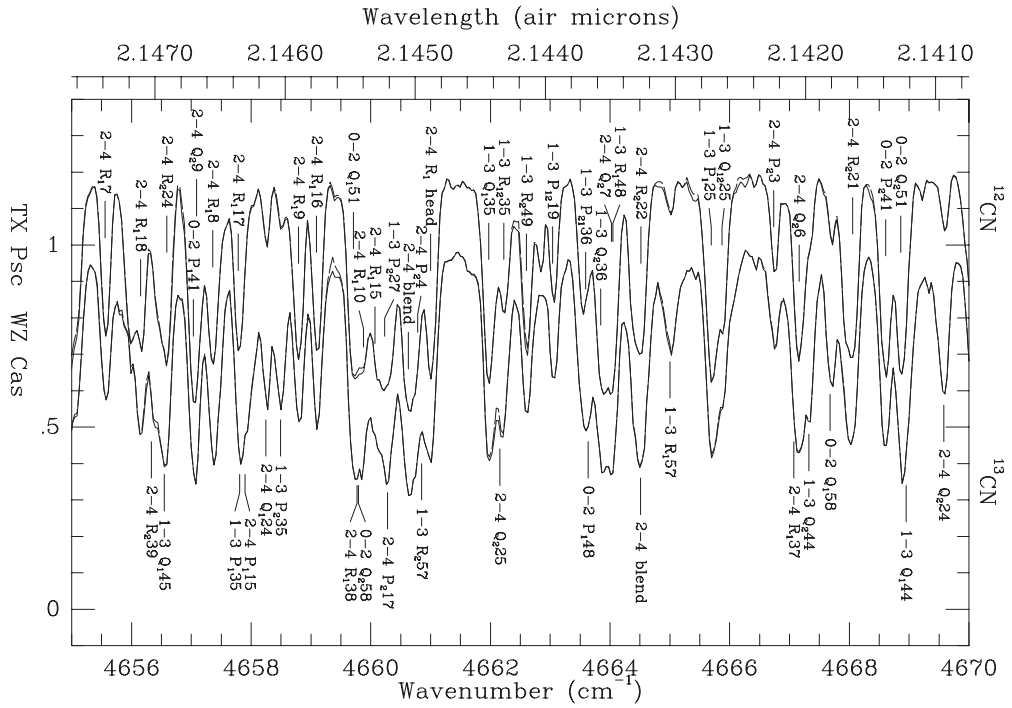

Figure 2. Spectra of two carbon stars in the region near 4662 cm^{-1}. TX Psc (above) has $^{12}C/^{13}C \sim 47$. WZ Cas (below) has $^{12}C/^{13}C \sim 4.5$. ^{12}CN lines are identified above the spectra and ^{13}CN below. Solid line, observed spectrum; dashed line, approximate correction for telluric absorption which is minor in this region.

Table 4
Equilibrium Constants (in cm^{-1}) for the $X\,^2\Sigma^+$ State of $^{13}C^{14}N$

Constants	$X\,^2\Sigma^+$
T_e	0.0
ω_e	2025.2513(16)
$\omega_e x_e$	12.5743(12)
$\omega_e y_e$	−0.00517(36)
$\omega_e z_e$	−0.000134(34)
B_e	1.820848070(95)
$\alpha_1 \times 10^2$	−1.630089(15)
$\alpha_2 \times 10^5$	−2.3301(61)
$\alpha_3 \times 10^7$	−3.473(73)
$\gamma_e \times 10^3$	6.9861(28)
$\gamma_1 \times 10^5$	−6.19(25)
$\gamma_2 \times 10^6$	−5.76(47)
r_e(Å)	1.171805675(31)

Note. Values in parentheses are one standard deviation uncertainties in the last digits.

1.23304088(36) Å and 1.171805675(31) Å for the $A\,^2\Pi$ and $X\,^2\Sigma^+$ states of $^{13}C^{14}N$.

5. COMPARISON WITH STELLAR DATA

Prior to the current work, some laboratory measurements were available for $^{13}C^{14}N$ bands in the >9000 cm^{-1} region. The current paper provides high-resolution measurements in the 4000–9000 cm^{-1} region. The completeness and improved frequency precision of our new line list should aid in identification of blended features in abundance analysis, determinations of isotopic ratios, and the identification of bands of less abundant molecules in this spectral region, especially in the complex spectra of carbon stars.

$^{13}C^{14}N$ red system lines have been identified in cool stars as early as K (see for instance Day et al. 1973). However, it is the spectra of the cool carbon stars that provide the richest CN spectra. These spectra provide a stringent test for any CN line list. The spectra at wavelengths short of 2 μm have a large number of saturated features and even continuum placement is difficult. The lines in the 2.0–2.5 μm region are less strong, although lines from CO, and C_2 are also present. This spectral region was previously used by Lambert et al. (1982) for abundance analysis. In Figure 2, we show a section of two spectra reported by Lambert et al. (1984). Spectra of a J-type carbon star with small $^{12}C/^{13}C$ (4.5, WZ Cas) and of an N-type carbon star with large $^{12}C/^{13}C$ (47, TX Psc) are shown. The J-type carbon stars have abnormally small $^{12}C/^{13}C$ ratio probably as the result of binary star interaction (Jorissen 2004). The large $^{12}C/^{13}C$ is the result of AGB mixing to the stellar surface of the products of CNO processed material (Lambert et al. 1984).

Using the line list for ^{13}CN provided here and the ^{12}CN line list from Ram et al. (2010) we have identified the lines in Figure 2. Clearly, the new line lists provide a highly complete set of identifications as well as provide excellent wavelength agreement between the stellar line positions and the line list. The wavenumber scales for the spectra have been adjusted to remove the heliocentric and intrinsic stellar velocities. The few telluric features present in this spectral region have been removed by reference to a telluric spectrum (Hinkle et al. 1995).

6. CONCLUSION

The emission spectra of the red system of $^{13}C^{14}N$ radical have been investigated at high resolution from the near-infrared to the visible region. A rotational analysis of 22 vibrational bands located in the 4000–15000 cm^{-1} region has been carried out and an improved set of spectroscopic constants has been obtained for the excited and ground states. The new measurements and spectroscopic parameters derived in this work should prove useful in the identification $^{13}C^{14}N$ molecular lines in stellar spectra of the 4000–10000 cm^{-1} region.

We thank J. Wagner, C. Plymate, and G. Ladd of the National Solar Observatory for assistance in recording and archiving the spectra. The National Solar Observatory is operated by the Association for Research in Astronomy, Inc., under contract with the National Science Foundation. This research made use of the SIMBAD database, operated at CDS, Strasborg, France as well as NASA's Astrophysics Data System Abstract Service. The research described here was partially supported by funds from the NASA laboratory astrophysics program. Some support was also provided by the UK Engineering and Physical Sciences Research Council (EPSRC).

REFERENCES

Amiot, C., Maillard, J. P., & Chauville, J. 1981, J. Mol. Spectrosc., 87, 196
Antipov, S. V., Sjölander, T., Nyman, G., & Gustafsson, M. 2009, J. Chem. Phys., 131, 074302
Banerji, M., Viti, S., & Williams, D. A. 2009, ApJ, 703, 2249
Bogey, M., Demuynck, C., & Destombes, J. L. 1984, Can. J. Phys., 62, 1248
Bogey, M., Demuynck, C., & Destombes, J. L. 1986, Chem. Phys., 102, 141
Brown, J. M., Colbourn, E. A., Watson, J. K. G., & Wayne, F. D. 1979, J. Mol. Spectrosc., 74, 294
Chen, Y., & Heaven, M. C. 2000, J. Chem. Phys., 112, 7416
Civiš, S., Šedivcová-Uhlíková, T., Kubelík, P., & Kawaguchi, K. 2008, J. Mol. Spectrosc., 250, 20
Day, R. W., Lambert, D. L., & Sneden, C. 1973, ApJ, 185, 213
Fay, T. D., & Wyller, A. A. 1970, Sol. Phys., 11, 384
Fray, N., Bénilan, Y., Cottin, H., Gazeau, M.-C., & Crovisier, J. 2005, Planet. Space Sci., 53, 1243
Garcia-Hernandez, D. A., Hinkle, K. H., Lambert, D. L., & Eriksson, K. 2009, ApJ, 696, 1733
Hause, M. L., Hall, G. E., & Sears, T. J. 2009, J. Phys. Chem. A, 113, 13342
Hempel, F., Röpcke, J., Pipa, A., & Davies, B. P. 2003, Mol. Phys., 101, 589
Hill, V., et al. 2002, A&A, 387, 560
Hirano, A., & Tsujishita, M. 1994, Appl. Opt., 33, 7777
Hinkle, K. H., Wallace, L., & Livingston, W. 1995, Infrared Atlas of the Arcturus Spectrum, 0.9–5.3 microns (San Francisco, CA: ASP)
Horká, V., Civiš, S., Špirko, V., & Kawaguchi, K. 2004, Coll. Czech. Chem. Commun., 69, 73
Hosinsky, G., Klynning, L., & Lindgren, B. 1982, Phys. Scr., 25, 291
Hosinsky, G., & Lindgren, B. 1976, A&AS, 25, 1
Hübner, M., Castillo, M., Davies, P. B., & Röpcke, J. 2005, Spectrochim. Acta, 61, 57
Jenkins, F. A., & Wooldridge, D. E. 1938, Phys. Rev., 53, 137
Johnson, J. R., Fink, U., & Larson, H. P. 1983, ApJ, 270, 769
Jorissen, A. 2004, in Asymptotic Giant Branch Stars, ed. H Habing & H Olofsson (New York: Springer), 461
Khachatrian, A., & Dagdigian, P. J. 2009, J. Phys. Chem. A, 113, 13390
Lambert, D. L. 1968, MNRAS, 138, 143
Lambert, D. L., Brown, J. A., Hinkle, K. H., & Johnson, H. R. 1984, ApJ, 284, 223
Liu, Y., Duan, C., Liu, H., Gao, H., Guo, Y., Liu, X., & Lin, J. 2001, J. Mol. Spectrosc., 205, 16
Maki, A. G., & Wells, J. S. 1995, Wavenumber Calibration Tables, NIST Database (NIST SP-118; Washington, DC: US Government Printing Office)
Mercier, X., Pillier, L., Pauwels, J.-F., & Desgroux, P. 2001, C. R. Acad. Sci., 2, 965
Meyer, D. M., & Jura, M. 1985, ApJ, 297, 119
North, S. W., Fei, R., Sears, T. J., & Hall, G. E. 1997, Int. J. Chem. Kinetics, 29, 127
Peach, G., Dimitrijevic, M. S., & Stancil, P. C. 2008, Proc. Int. Astron. Union, 4, 385
Prasad, C. V. V., & Bernath, P. F. 1992a, J. Mol. Spectrosc., 156, 327
Prasad, C. V. V., & Bernath, P. F. 1992b, J. Mol. Spectrosc., 151, 459
Ram, R. S., Davis, S. P., Wallace, L., Engleman, R., Appadoo, D. R. T., & Bernath, P. F. 2006, J. Mol. Spectrosc., 237, 225
Ram, R. S., Wallace, L., & Bernath, P. F. 2010, J. Mol. Spectrosc., 10, 95
Rehfuss, B. D., Suh, M.-H., Miller, T. A., & Bondybey, V. E. 1992, J. Mol. Spectrosc., 151, 437
Riffel, R., & Pastoriza, M. G. 2007, ApJ, 659, L103
Roth, K. C., Meyer, D. M., & Hawkins, I. 1993, ApJ, 413, L67
Sansonetti, C. J. 2007, J. Res. Natl. Inst. Stand. Technol., 112, 293
Smith, V. V., et al. 2002, AJ, 124, 3241
Tamaoki, M., Yamauchi, Y., & Nakai, H. 2005, J. Comput. Chem., 26, 436
Titarchuk, T. A., & Halpern, J. B. 1995, Chem. Phys. Lett., 232, 192
Turner, B. E., & Gammon, R. H. 1975, ApJ, 198, 71
Wang, M., Henkel, C., Chin, Y.-N., Whiteoak, J. B., Cunningham, M. H., Mauersberger, R., & Muders, D. 2004, A&A, 422, 883
Whaling, W., Anderson, W. H. C., Carle, M. T., Brault, J. W., & Zarem, H. A. 2002, J. Res. Natl. Inst. Stand. Technol., 107, 149
Wiedemann, G. R., Deming, D., Jennings, D. E., Hinkle, K. H., & Keady, J. J. 1991, ApJ, 382, 321
Wootten, A., Lichten, S. M., Sahai, R., & Wannier, P. G. 1982, ApJ, 257, 151
Wyller, A. A. 1966, ApJ, 143, 828